J Therm Anal Calorim (2010) 99:337–348
DOI 10.1007/s10973-009-0137-x

Calorimetric and spectrophotometric investigation of PLGA nanoparticles and their complex with DNA

Mariam Khvedelidze · Tamaz Mdzinarashvili · Tamar Partskhaladze · Noha Nafee · Ulrich F. Schaefer · Claus-Michael Lehr · Marc Schneider

Received: 28 October 2008 / Accepted: 26 May 2009 / Published online: 13 August 2009

Abstract The calorimetric investigation of non-coated and chitosan-coated PLGA nanoparticles (NP) shows that at initial temperatures of heating particle swelling takes place what results in an internal architectural change at lower than physiological temperature. It has shown that the temperature of NP tightness perturbing depends on solvent polarity: as more polar is the solvent more stable are particles. The break of existing bonds in NP shell is accompanied with heat absorption peak which undergoes significant changes depending on heating rate. In the wide pH 2–8 interval in transition temperature no changes occurred. The obtained results show that such NP could be used in acidic area for drug transfer, which gives possibility to take medicine orally. It was shown that DNA attaches only to chitosan-coated NP. The optimal ratio for DNA loading onto the NP was found to be 7:1 (W_{NP}/W_{DNA}).

M. Khvedelidze · T. Mdzinarashvili (✉) · T. Partskhaladze
Department of Physics, Faculty of Exact and Natural Sciences, Ivane Javakhishvili Tbilisi State University, 3, Chavchavadze Ave., 0128 Tbilisi, Georgia
e-mail: mdz@tsu.ge

M. Khvedelidze · T. Mdzinarashvili
Institute of Molecular Biology and Biophysics, 12, Gotua Str., 0160 Tbilisi, Georgia

N. Nafee · U. F. Schaefer · C.-M. Lehr
Biopharmaceutics and Pharmaceutical Technology, Saarland University, Postfach 151150, 66041 Saarbrücken, Germany

M. Schneider
Pharmaceutical Nanotechnology, Saarland University, Postfach 151150, 66041 Saarbrücken, Germany

Keywords Calorimetry (DSC) · Nanoparticles · Spectrophotometry · Drug delivery systems · PLGA · Nanoparticles DNA complexes

Introduction

Modern pharmaceutical approaches have allowed to identify many potent drugs. Unfortunately, many of those show a small bioavailability because of their limited aqueous solubility. Hence, NP offer the potential to overcome not only this obstacle but also promise smaller amounts of drugs delivered to specific cells and tissues [1–3]. Also the perspective of using NP is very interesting when the problem is to deliver the therapeutic agents to the damaged organ or tissue unaltered, crossing natural barriers which are the first obstacle for drug delivery. For a broad applicability the consideration of diverse environmental conditions such as high acidic pH, unfavorable metal ions, active enzymes, etc. are essential. Nanotechnology is considered to inherit a huge potential for drug delivery, since it offers a suitable transportation of anticancer agents, antihypertensive agents, immunomodulators, hormones, and macromolecules such as proteins, peptides, antibodies or genes [1–12].

Recently, NP with a therapeutic agent of interest encapsulated in their polymeric matrix or adsorbed or conjugated onto the surface [1, 13–28] can be administered orally or injected locally [23, 25, 29]. One of the most common NP is made of poly (lactic acid) (PLA) [30], poly (glycolic acid) (PGA), and their copolymers poly (lactic-co-glycolic acid) (PLGA) [25, 31–39]. Such polymers have controllable biodegradability, excellent biocompatibility, high safety, they are non-toxic, and they are restorable through natural pathways [34, 40–46]. One disadvantage of

existing delivery systems is the limitation by using organic solvents and relatively harsh formulation conditions. PLGA NP are generally formulated using emulsion solvent evaporation or by solvent displacement techniques [33], which induce some problems with limited core loading, i.e., <15%, the variable burst release of entrapped drug and organic solvent residues [47]. One of the main drawbacks of colloidal carriers is that they tend to agglomerate during storage. Therefore it is important to determine the structural changes which take place in NP shell. There are literary data indicating that the drug entrapped in PLGA matrix is released at a sustained rate through diffusion of the drug in the polymer matrix and by swelling and degradation of the polymer matrix [32, 47, 48], though there has not been studied completely the mechanism by which the drug entrapped in such NP releases in time.

Hedley et al. have demonstrated protection of DNA from nucleases when encapsulated into PLGA microspheres [49]. By changing the copolymer composition and molecular weight it is possible to vary the release of encapsulated drugs from PLGA NP from days to months [1, 33, 35, 50–55]. There are literary data confirming that DNA can be condensed on dendrimers [56, 57], cationic peptides [58, 59], cationic polymers [60–67], cationic lipids [68–72], as well as on liposomes [47, 73–80]. DNA could be transferred to the cells encapsulating in or by adsorption onto the particles surface [54, 55, 69, 81–84]. These properties are the reason for PLGA being approved by the FDA [33].

Chitosan is a promising and often used candidate for surface modification due to its biocompatibility and its positive charge [85]. Chitosan-modified PLGA should adsorb better than other lipophilic polymer derivatives, because of its hydrophilicity, and improve transfection rate of the particle–DNA complexes in vitro and also in vivo experiments [86].

For successful application of NP as gene delivery systems their interaction with the payload is essential. Therefore a fundamental study was performed regarding NP and their possible biological active complexes. From this point of view it is important to investigate the influence of each possible environmental parameter on NP–DNA complexes. The goal of our study was the biophysical investigation of the physico-chemical properties of PLGA NP. Especially, the examination of the influence of environmental conditions (pH, temperature, polarity of the solvent) on the NP behavior and their interaction with DNA was investigated. For this reason two types of NP have been chosen to study: non-coated and chitosan-coated NP with the main size 148.2 nm and 146.8 nm, respectively. These two almost the same sizes nanoparticle (but with different charges) have been chosen for study the influence of potential on stability and interaction possibility with DNA at different environment conditions.

Materials and methods

Non-coated and chitosan-coated PLGA NP were made using solvent evaporation methods [83, 87–89]. In brief, PLGA 70:30 was dissolved in 5 mL ethyl acetate at room temperature. The organic phase was added dropwise to an equal volume of the aqueous phase, containing the stabilizer PVA (2.5% w/v) for PLGA particles and PVA and chitosan for chitosan-coated particles (cNp), under stirring using a magnetic stirrer, at 1000 rpm, for 1 h, at room temperature. The emulsion was then homogenized (Ultra-Turrax T25, Janke & Kunkel GmbH & Co-KG, Germany) at 13,500 rpm for 10 min. Nanoprecipitation was performed by adding MilliQ water dropwise under gentle stirring to obtain a final volume of 50 mL. Stirring is continued overnight at room temperature to get rid of the organic solvent. The size distribution of the particles was determined using photon correlation spectroscopy. The non-coated PLGA nanoparticle (nNP) size was found to be $d = 148.2$ nm (PI = 0.03, charge −8.6 mV). In the case of chitosan-coated PLGA NP (cNP) the size was 146.8 nm (PI = 0.12, charge +39.98 mV).

Calf thymus DNA (Sigma) has been chosen to investigate the particles interaction with nucleotides. All degrading influences such as contact of the sensitive DNA with extreme pH values or organic solvents during the preparation process were avoided because DNA was added after all other preparation steps were finished.

The study of the thermodynamic features of PLGA NP and the interaction between DNA and the NP were carried out using a precise DASM-4A microcalorimeter (Russian Academy of Science, Pushchino, Russia), which belongs to high sensitivity type heat flow calorimeters [90]. In addition, this device allows to carry out experiments with low rate of temperature scanning and therefore to perform quasi equilibrium measurements. The spectrophotometric investigation was done using the spectrophotometer HEλIOS β (Thermospectronic, Thermo Fisher Scientific, USA). The centrifugation of NP was accomplished using the Beckman Coulter™, Allegra™ 64R Centrifuge and particle sedimentation was accomplished at 18,000 rpm (23183 g). The device of turbidity was constructed in Tbilisi State University by us, where as a source of light it is used blue light-emitting diode (with wavelength $\lambda = 480$ nm) and the detector of light is photomultiplier.

Results

For nanoparticle application in biological systems it is important to investigate their stability under different environmental conditions such as temperature, pH, various salts, etc. The thermodynamical properties of NP have been

studied to gain some insights about nanoparticles' properties using supersensitive differential microcalorimetric method.

To calculate nanoparticle specific heat capacity it is necessary to know nanoparticle partial volume. According to nanoparticle weight, diameter and its shape, we calculated the partial volume. NP in water were situated in suspended condition and had a spherical shape with approximately 147 nm diameter [89]. This allows to calculate the nanoparticle volume which turned out to be on average 1.7×10^{-15} cm^3. Based on nanoparticle mean weight which is 2.88×10^{-15} g, finally, it is possible to calculate the nanoparticle partial volume which turned out to be $v = 0.59$ cm^3 g^{-1} (or density $\rho = 1.695$ g cm^{-3}).

In Fig. 1 the chitosan-coated PLGA nanoparticle (a) and non-coated nanoparticle (b) suspension microcalorimetric fits are shown. The heating rate was 2 °C min^{-1}. As it is seen from calorimetric recording the curves have difficult form, but for both particles have the same appearance. Therefore hereinafter we give only the results for the thermodynamic parameter investigation for one of the NP, as the results were basically identical for equal conditions.

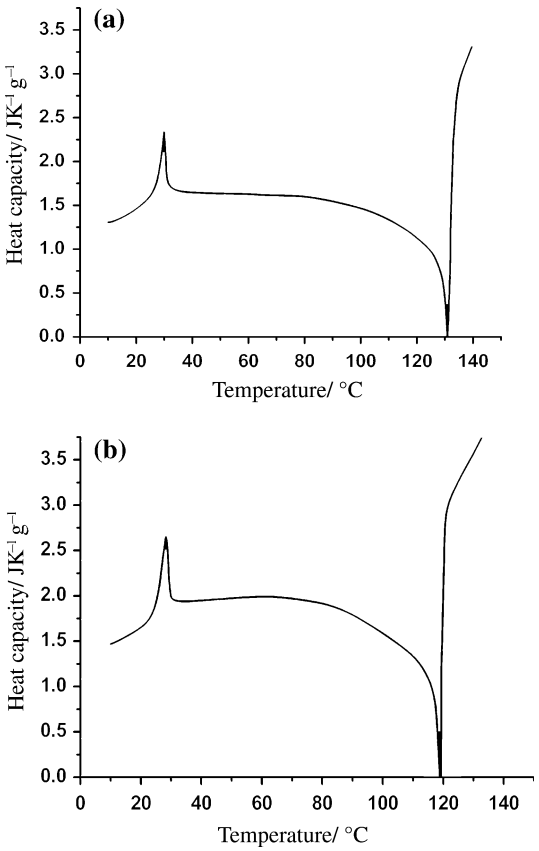

Fig. 1 Dependence of the specific heat capacity on temperature: **a** in the case of chitosan-coated PLGA nanoparticles; **b** in the case of non-coated PLGA nanoparticles. The heating rate was 2° min^{-1}. Solvent was bidistilled water, pH 5.0

From the microcalorimetric curve four temperature intervals can be concluded: (a) 10–23 °C; (b) 23–35 °C; (c) 35–130 °C; (d) 130–140 °C. The heat capacity increase in 10–23 °C temperature interval during temperature rise is due to the fact that the volume of nanoparticles' increases (Fig. 1). As the DASM microcalorimeters measure the heat capacity of investigated solution with constant volume, so even the negligible rising of nanoparticles' volume causes the changes in heat capacity value of nanoparticles' solution which we have observed in our experiments. As it can be seen the subsequent increasing of temperature leads to swelling and the stretching of particles' surface and in 23–35 °C temperature interval the particles' ordered structure change occurs and its core becomes reachable for the solvent. The phase transition temperature T_m for the chitosan-coated NP is 30 °C and in the case of non-coated NP is 28 °C. The enthalpy of this peak of heat absorption in both cases is in order of 2 J g^{-1}. Furthermore, at elevated temperatures ($T_m > 50$ °C) the monotonously decreasing curves indicate that the particles start to aggregate (Fig. 1). Further increasing of the temperature leads to particles' aggregate destruction (above 120 °C) which appears in sharp increase of particles' heat capacity.

It was carried out turbidity measurements of NP with temperature (non-coated; PLA/PLG 70:30). The suspension of NP was placed in the glass tube with length 10 cm, which was heated by heater which was surrounded around tube. The measurement of temperature was carried out by mercury thermometer, which with good thermal contact was fixed on the glass tube. On the Fig. 2 it is given dependence of suspension transparency changes on temperature during scanning the temperature, from which it is obvious that while increasing the temperature of NP in 15–35 °C temperature interval the intensive suspension transparency increase takes place (heating of suspension up

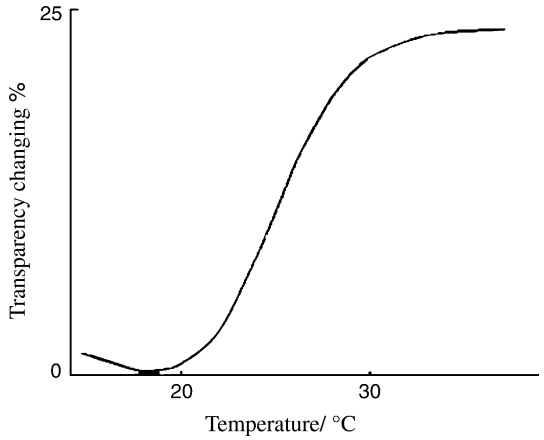

Fig. 2 Dependence of noncoated nanoparticles' suspension transparency on heating temperature

to higher temperatures (>50 °C) was not achieved for this time due to construction of device).

Spectrophotometric data revealed that the so-called Rayleigh scattering (light intensity is proportional to λ^{-4}) is the same for both, "native" particles and particles after heating them till 150 °C and cooled then down (Fig. 3). In other words, the absorption spectrum of the destroyed chitosan-coated NP, obtained by heating up to 150 °C, did not differ from the spectrum of the "native" ones. The same results were obtained for non-coated NP.

To determine whether the NP melting is a kinetic process or not, the calorimetric experiments with NP suspensions at different heating speeds (0.5, 1, 2, 4 °C min^{-1}) have been carried out (Fig. 4). These experiments show that the thermodynamic parameters such as T_m and the particle break-up enthalpy (the area of the peak in 23–35 °C temperature interval) depends on particle heating rate. In particular, the higher the speed of heating, the higher is the particle transition temperature T_m and their melting enthalpy (Table 1).

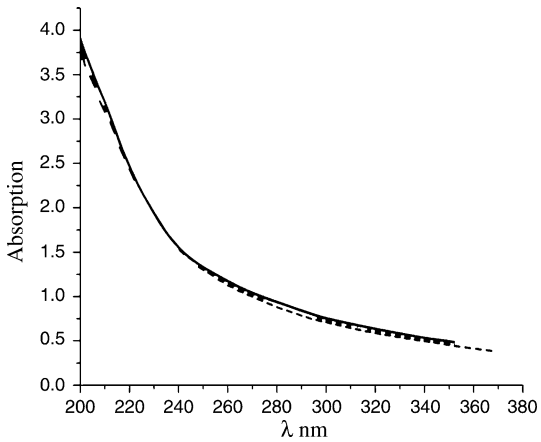

Fig. 3 The light absorption spectra of chitosan-coated PLGA nanoparticles (the solid line) with 1.238 mg mL^{-1} concentration and for denatured particles with the same concentration (the dash line). Solvent was bidistilled water, pH 5.0

Table 1 Dependence of transition temperature (T_m) and melting enthalpy (ΔH) of non-coated PLGA nanoparticles on the different heating rates

Heating rate V/°C min^{-1}	Transition temperature T_m/°C	Melting enthalpy ΔH/J g^{-1}
0.5	26.5	1.87
1	27.9	1.92
2	29.5	1.98
4	31.7	2.25

In addition, the experiments have been carried out with the so-called nanoparticle, annealing by temperature, where NP were heated only till 23 °C—the temperature where the NP internal architecture is starting to modify (Fig. 5), and then the calorimeter was turned to cooling regime. The peak is restored at lower temperature (T_m = 25 °C) after particle reheating and enthalpy of this peak is also decreased (approximately three times). According to Fig. 5 the particles change occurs at lower temperature (the particles, heated until 23 °C, were already modified) than in this case of heating "native" once, where the T_m = 30 °C (see Fig. 1a).

For practical application it is important to determine the storage stability of the NP. Especially, the storage in suspension for these biodegradable samples is of high interest. For this reason the calorimetric experiments with nanoparticle prepared 3 months before and stored at 4 °C in refrigerator were carried out. The result was compared with the same experiment performed with freshly prepared particles. Figure 6 shows calorimetric curves for freshly prepared non-coated NP (line 1) and the same

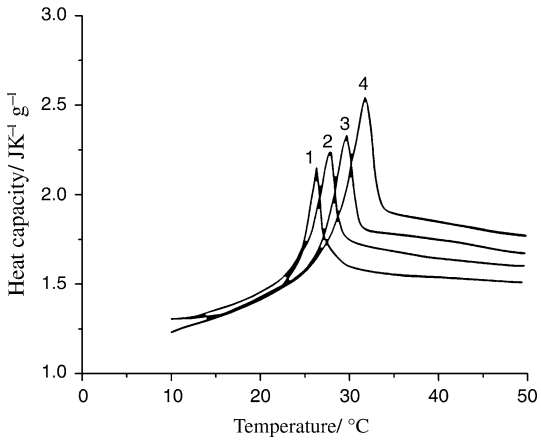

Fig. 4 Dependence of the specific heat capacity of non-coated PLGA nanoparticles on temperature at different heating rates: 1—0.5, 2—1, 3—2, 4—4 K min^{-1}

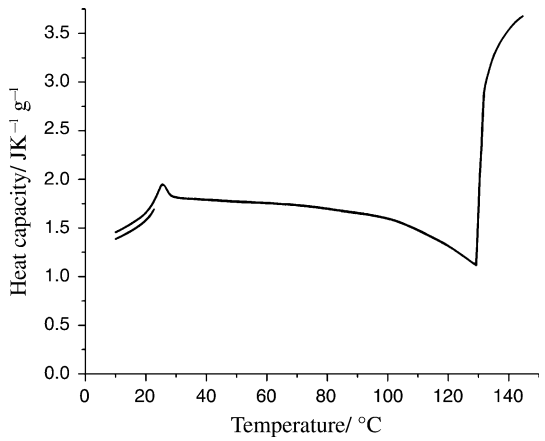

Fig. 5 Dependence of the specific heat capacity of non-coated PLGA nanoparticles on temperature: first heating till 23 °C; second is the totally heating up to 150 °C

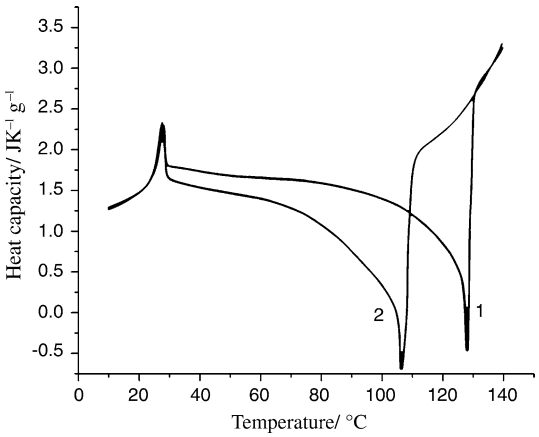

Fig. 6 Dependence of the specific heat capacity of non-coated PLGA nanoparticles on temperature: 1—fresh prepared nanoparticles; 2—the nanoparticles after 3 months

particles after 3 months (line 2). As it can be seen from this figure storage time influences only particle aggregation process, in other words, the influence of time on NP becomes apparent in an attempt to increase particle aggregation (they aggregate at lower temperature: in 40–110 °C range).

It is known that in creation of nanoparticle existence of hydrophobic forces play an important role. Therefore, we changed the solvent's polarity to investigate the solvent–particle interaction. The calorimetric experiments in 10% ethanol solution lead to a decreased the transition temperature to $T_m = 24$ °C (Fig. 7). In contrast to water, in ethanol no aggregation was observed. Moreover, because of the reduced solvent hydrophobicity no particle aggregation process was observed.

As it was mentioned above, under the influence of temperature, at first NP widening (10–25 °C) takes place, which is followed by the particle cracking process at

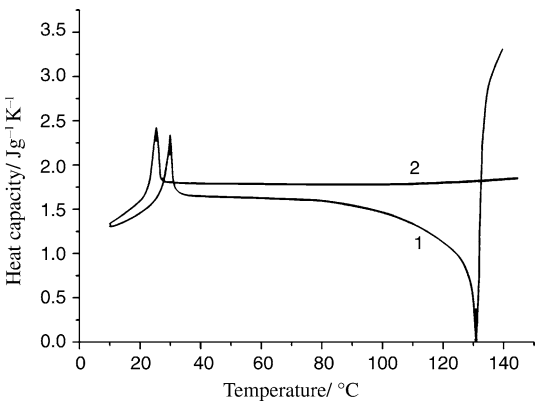

Fig. 7 Dependence of the specific heat capacity of chitosan-coated PLGA nanoparticles on temperature: 1—nanoparticles in bidistilled water; 2—nanoparticles in 10% methanol solution

$T_m = 30$ °C. Hence the particle transition temperature has to be depended on the environmental pressure. In all our calorimetric experiments the samples were situated under 6–7 atmosphere pressure to avoid the solution boiling process during the heating. To find out if the pressure influences on widening process, the experiments have been performed at 1.5 and without excess pressure. No differences were obtained.

We consider that the knowledge of polymer solution behavior is necessary to improve understanding of micro sphere formation and drug micro encapsulation. Obviously, the purpose of these experiments was to determine the role of deionized water in the stability of NP. Our results emphasize that using deionized water is not so necessary for stability of nanoparticle. For this reason other parameters such as the solvent's pH were investigated. Figure 8 shows microcalorimetric study of NP in buffers of different acidity ranging from pH 2 to 8.2. The buffer molarity was chosen not too low (0.02 M Na_2HPO_4 and 0.01 M citric acid) to obtain a sufficient buffer capacity for maintaining the solution's pH during the heating process in the wide temperature interval (10–150 °C). These data are compared to the calorimetric data of NP suspension in pure bidistilled water.

To determine the interaction of PLGA non-coated NP and chitosan-coated NP with DNA the calorimetric, ultracentrifuge and spectroscopic methods were applied. The calorimetric experiment was carried out using mixture of DNA and chitosan-coated NP solution, which shows that the heat absorption peak is constricted in the case of DNA presence in particles' solution, what biophysically means that interaction between them takes place (Fig. 9). In this experiment the nanoparticle/DNA ratio was 1200:1 (w/w). At higher DNA concentrations aggregates appear in solution which made the calorimetric investigation impossible.

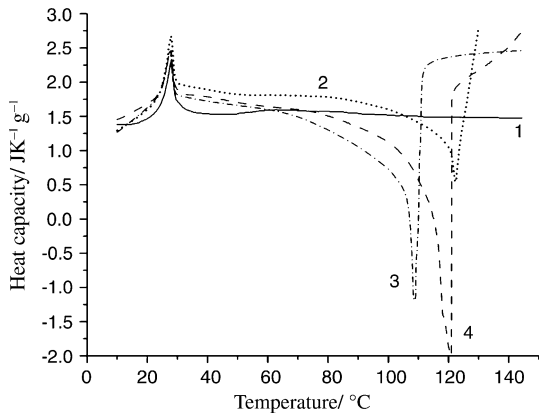

Fig. 8 The microcalorimetric study of chitosan-coated PLGA nanoparticles, immersed in buffers with different acidity, ranging from pH 2 to 8.2. The buffer molarity was 0.02 M Na_2HPO_4 and 0.01 M citric acid. The solid line—pH 2; the short dot line—pH 3.8; short dash dot line—pH 5; dash line—pH 8.2

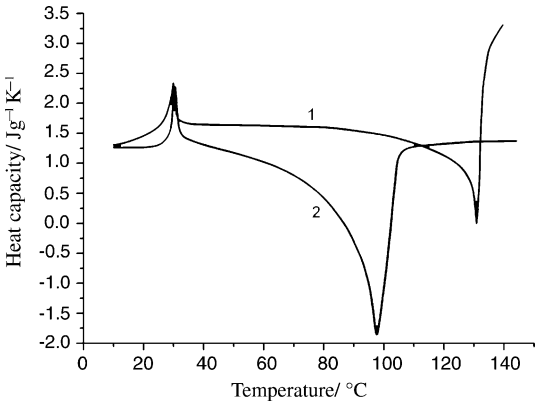

Fig. 9 Dependence of the specific heat capacity of chitosan-coated PLGA nanoparticles on temperature: 1—the calorimetric curve of chitosan-coated nanoparticles; 2—the complex of chitosan-coated nanoparticles with DNA at 1200:1 (w/w) nanoparticles/[DNA] ratio. Solvent: bidistilled water, pH 5.0

In the case of interaction between non-coated NP and DNA we haven not observed complex formation even when the ratio was 24:1. The width of heat absorption peaks were the same in both cases (Fig. 10), in contrast to the mixture of DNA and chitosan-coated NP (see Fig. 9). After the heat absorption peak, approximately in the temperature interval from 40 to 100 °C, the values of heat capacity are parallel to the temperature axis, what means that there is no aggregation process between the destroyed particles in this temperature interval. The aggregates originate at 100–140 °C and at higher temperatures the destruction process of aggregates to simple particles is observed.

For more exact determination of DNA–particle interaction the spectrophotometric and ultracentrifugation methods were used. Foreseeing the contribution of

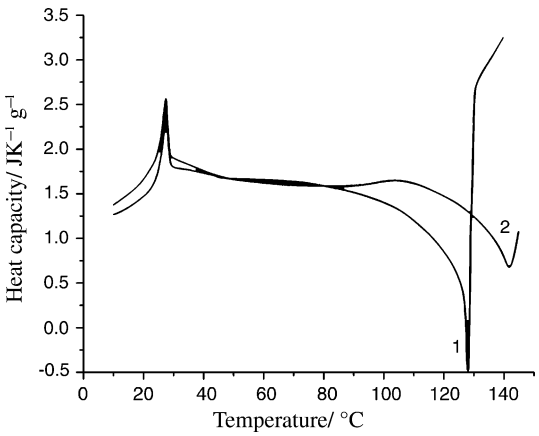

Fig. 10 Dependence of the specific heat capacity of non-coated PLGA nanoparticles on temperature: 1—the calorimetric curve of non-coated nanoparticles; 2—the complex of non-coated nanoparticles with DNA at nanoparticles/[DNA] ratio 24:1 (w/w)

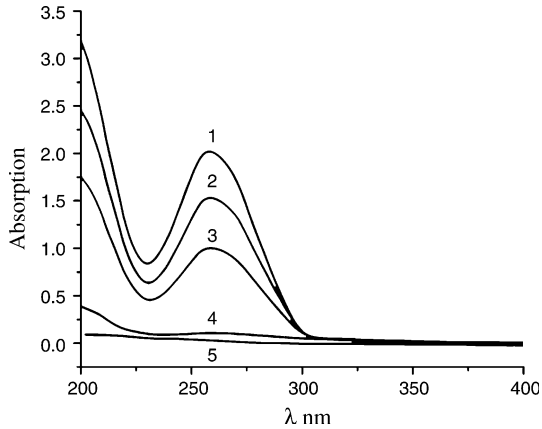

Fig. 11 The dependence of DNA–chitosan-coated nanoparticle solution absorption on wavelength at different nanoparticles/[DNA] ratios: 1—0; 2—1.685; 3—4.045; 4—6.726; 5—11.37

chitosan-coated NP in spectrum, the spectra of pure DNA with the spectrum of the same concentration DNA plus chitosan-coated NP have been compared. We had the next idea: if DNA interacts with NP so the DNA have to be attached with NP and during sedimentation the complex would fall away to bottom. The dependence of DNA absorption on wave-length at various NP/[DNA] ratios is given in Fig. 11. As it is evident from this figure at the beginning when the nanoparticle concentration is zero or pure DNA spectrum is present in the solution (curve 1). By adding chitosan NP to DNA solution and measure the sample after centrifugation shows that the value of absorption is decreased which is caused by the reduction of free DNA due to adsorption onto the particles' surface. For high chitosan–NP concentrations DNA is adsorbed completely onto the particles, whereas in the case of DNA interaction with non-coated NP, the spectrophotometric experiments did not reveal such interaction. Figure 12 shows the dependence of DNA-non-coated nanoparticle solution absorption on the wavelength at the same NP/[DNA] ratios.

To determine the amount of DNA which can be adsorbed on the surface of the NP the dependence of the number of NP was plotted against the DNA mass unit. Figure 13 depicts the absorption at 260 nm (maximal value for each sample) at various chitosan-coated NP/DNA (solid line) and non-coated NP/DNA (dotted line) ratios. As it is seen from the curve of DNA-chitosan nanoparticle complex (solid line) when cNP/DNA ratios higher than 7, the whole DNA is associated with chitosan-coated NP. When these ration is <7, DNA molecules appear in solution which are not able to connect with NP any more, because the particles surface is already saturated with DNA molecules. At the end (onset diagram) we have the value of absorption for pure DNA (2 OD) in the solution. The optimal number of chitosan-coated NP, which could complex with DNA,

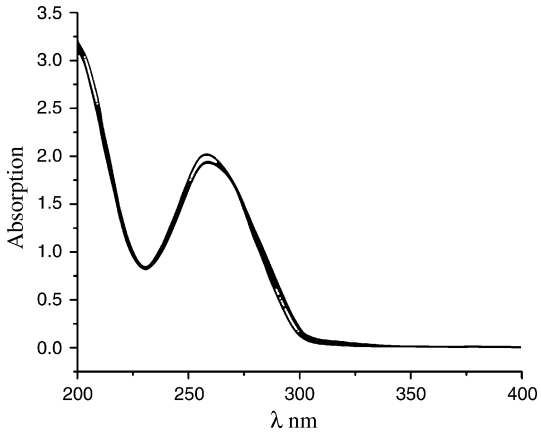

Fig. 12 The dependence of DNA-non-coated nanoparticle solution absorption on the wavelength at different nanoparticles/[DNA] ratios: 1—0; 2—1.685; 3—4.045; 4—6.726; 5—11.37

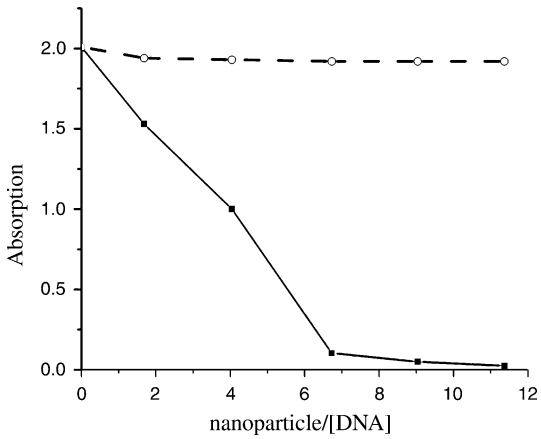

Fig. 13 The dependence of DNA-nanoparticle solution absorption at 260 nm wavelength on nanoparticles/[DNA] ratio in the case of chitosan-coated nanoparticles (*solid line*) and non-coated nanoparticles (*dotted line*)

could be extrapolated from those curves. Finally, we conclude that the optimal ratio of chitosan-coated NP to DNA is 7:1 (w_{Np}/w_{DNA}).

Discussion

From the calorimetric results in Fig. 1 we can conclude that the coating of NP with chitosan did not exert an influence on the behavior of the particles. The thermodynamic parameters, in particular the profile of temperature dependence of the specific heat absorption curves for non-coated NP and chitosan-coated NP were the same. Also it is clear that the calorimetric curves themselves have a complex shape (Fig. 1) which is composed out of the heat absorption peak area (23–35 °C), the sharp change at $T \sim 130$ °C, and the monotonic sections from 10–23 °C and 35–130 °C. Such complicated nature of the calorimetric curves indicates that the temperature has multifarious influences on the NP and causes significant modification of their structure. It should be mentioned that the influence of temperature on NP starts right at the beginning of the experiment, namely at 10 °C, where an increasing heat absorption is observed which turns into a peak at 23–35 °C temperature interval. At the beginning of the experiments, respectively, at the start of temperature scanning the increase of particle specific heat absorption might be induced by increasing the particle volume, as it happens typically for solid bodies. We reach a such conclusion, owing to the calorimetry construction, because the DASM-4A calorimeter is a device whose ampule is represented by platinum thin capillary which when it is entirely infilled, measures the sample heat effect for only the half of the filled volume. Other construction calorimeters (calorimeters, whose measuring ampules are hermetically closed) measure the whole investigated sample heat effect and are less sensitive to particle widening effect [91]. In other words, as we have mentioned above, in our case the DASM-4A calorimeter measures only part (half) of the suspension filled up in the capillary and if the volume of the particle changes in this part of the capillary, this change instantly effects the heat capacity of this volume phase. Moreover, based on aforesaid it is clear that in such calorimeters it becomes necessary to know the partial volume for measuring the sample's heat capacity, which we have calculated above. Finally it can be concluded, that at initial temperatures the particle volume increase takes place, the particle swelling, which at 23–35 °C temperature interval finishes with particle cracking. Because in this case the break in particle existing bonds takes place, the heat absorption peak is springing up. Obtained by turbidity measurements curve (Fig. 2) should be related with volume increase of spherical NP (in mentioned temperature interval) until it will be destroyed, as a result of this (>30 °C) the transparency of suspension is changed not considerably. We would like to underline the circumstance, that while increasing the temperature of suspension the small (not large) increase of nanoparticles' volume takes place, which results the decrease of concentration of NP in suspension (the number of particles in the unit of volume will be less) and consequently the increase of turbidity occurs. This experimental datum is explaining the increase of specific heat capacity of NP in the above mentioned temperature interval which takes place during calorimetric experiments. On the other hand it should be mentioned that the shape and also the size of the NP did not change even for such high temperature as 150 °C, because cooling them back to room temperature give us the homogeneous suspension which absorption spectrum is analogous

to the spectrum of non-heated nanoparticle suspension. This is supported by spectrophotometric data showing the so-called Rayleigh scattering (the scattering intensity $I \sim \lambda^{-4}$) which is the same for "native" and destroyed particles (Fig. 3). Moreover, the spectrum of the destroyed particles, obtained by heating up to 150 °C, did not differ from the spectrum of the "native" particles or they are just cracked by heating. This indicates that the particles (polymer composition) themselves are coctostabile; otherwise they would be destroyed entirely at high temperatures. Therefore the optic spectroscopy, in particular turbodimetric method, is not able to distinguish the initial and temperature-induced changed NP from each other. After particle cracking at 30 °C, from our point of view, on the surface of cracked particles additional hydrophobic chemical groups are exposed which avoid water molecules and try to connect with the neighbouring particle surface hydrophobic groups. It betokens that particles will aggregate. From calorimetric curve we can see that after the heat adsorption peak, at higher temperature the specific heat capacity curve is decreasing approximately from 50 to 120 °C area (Fig. 1), which is the typical case of aggregates appearing. A further increasing of temperature (above 120 °C) leads to a sharp increase of the heat capacity curve, and we suppose that it is caused by aggregate/conglomerate dissociation, perhaps to suspension of NP. The hydrophobic part of torn NP falls into the contact with water and with further temperature increase the amount of aggregates raises.

The herein described approaches to characterize PLGA nanospheres may help the formulation scientists to become aware of the complexity of this process and understand it better. Also it should be mentioned that one of our purposes was to study of possibility using chitosan NP for DNA delivery, because they can complex anionic DNA on the surface of the NP to obtain gene carriers. We suppose that it does not matter would NP be closed or broken circuit, DNA is able to fold over the surface of both type of particle. Therefore the chitosan-coated PLGA NP with PLA/PGA ratio 70:30 could be used for this purpose.

Experimental data of Fig. 4 points out that particles destruction does not occur instantly and this process is stretched in time. The obtained thermodynamical results point out that the nanoparticle destruction process is not equilibrium. The particle destruction degree depends on the heating rate, because there are different values for enthalpy and specific heat capacity of NP at different heating rates. The minimal heating rate of existing scanning calorimeter is not enough for determining the tightness breaking equilibrium temperature. Earlier it has been shown that PLGA (50:50) NP, with inherent viscosity of 0.69 dL g^{-1} coated with PVA, have glass transition temperature (T_g) onset 38 °C and endset 45 °C [91]. The heating speed in those calorimetric experiments was 10 °C min^{-1}. Because of thermal gradients, the high heating rate caused the transition temperature value increase. In other words, the closer we can come to equilibrium the exacter the thermal parameters can be measured.

This is also supported by the so-called annealing experiments where NP first were heated only until 23 °C (Fig. 5). The significant changes in the enthalpy and transition temperature (T_m) from 30 to 25 °C in the reheating curve show that if the particles are heated till the temperature, which is required to start their internal transition, the process proceeds spontaneously—no more energy is needed to destroy them up to the end. This result would be absolutely understandable, if the particles would be destroyed under the influence of temperature and they could not restore their "native" structure. This experiment show that the particles destroy equilibrium temperature is less than 23 °C because after stopping temperature scanning in calorimeter, during that little time while the temperature of suspension was 23 °C the significant decrease of nanoparticle stability takes place (Fig. 5).

The results of Fig. 6 confirm once more that the particles are unbroken and there is no inside solution leaking from such particles by diffusion as it was indicated in literary data [32, 47, 48]. Otherwise there must be the differences in recording between freshly prepared nanoparticle and particle properties after some months at low temperature interval (10–40 °C) in calorimetric curves where the heat absorption peak is observed and time influences only on particle aggregation process.

It is clear that the existence of hydrophobic forces in creation and stability of nanoparticle emphasizes the high profile. The NP destruction temperature depends on the contact forces which originate during production. The main part belongs to hydrophobic forces. However, their strength depends on the solvent properties around the particles. Changing (decrease) the polarity of the solvent would have significant influence (diminution) on particle transition temperature. In other words the stability of the particles must depend on the extent of solvent's polarity. In Fig. 7 we can see T_m of the particles' diminished right away (from 30 up to 24 °C) when a 10% ethanol solution is used. Moreover because of the solvent's hydrophobicity decrease there was no particles' aggregation process observed.

An important parameter for future applicability of NP-based delivery systems in pharmaceutics is their stability under relevant environmental conditions to avoid their damage and prematurely drug release. Therefore, the influence of temperature, pH and various salts on NP needs to be investigated. At first, an unchanged T_m (Fig. 8) indicates the stability of the NP in all investigated pH-values. The NP maintain their structure in deep acid (pH 2)

as well as in alkaline (pH 8.2) conditions (heat absorption peak at 30 °C, Fig. 8), i.e. the particles are not destructed under these conditions. Moreover, the constant heat capacity in the acid range for $T > T_m$ reflects the augmented stability due to electrostatic repulsion, in contrast to water and alkaline ranges. This is valid and expected for chitosan-coated NP. For non-coated NP this would be surprising because of the absence of any pH influence [91]. Therefore besides the particles are stable in buffer, in pH 2 (stomach pH) there is no aggregation process observed. The experiments unambiguously show that in a wide pH interval (2–8) the changes in transition temperature did not take place. These results are important for two reasons: such NP (PLA/PGA ratio in these PLGA NP is 70:30) could be used in acidic surrounding (for instance, in stomach) for drug transfer and the particles structure, stability and their other properties are less depended on either the particles were in water (bidistilled or deionized) or the suspension of particles were located in buffer (at least in buffer with low molarity).

For determination the interaction between DNA and NP calorimetric experiments have been carried out. For non-coated NP no interaction with DNA was observed spectrophotometrically, independently on the mixing ratio (Fig. 10). This is not surprising, because of the negative charge of both components. However, there is a difference between non-coated NP and DNA-non-coated nanoparticle complex calorimetric curves in the high temperature regime. This means that negatively charged particles aggregation temperature interval is rather moved towards higher temperatures (>120 °C, Fig. 10) as in the interval of 30–110 °C NP aggregation did not occur.

When DNA was added to chitosan-coated NP suspension aggregates appeared in solution, what unambiguously points to arising of complex between DNA and NP due to electrostatic attraction between negatively charged phosphate groups of DNA molecule and positively charged chitosan-coated NP. This complex springs up in such way that the DNA wraps around such particles. The loading of the particles limited only for small quantities of DNA or better at high ratios of cNP/DNA ($\sim$1200:1). For smaller ratios aggregates were observed in solution (Fig. 9). In spite of such little amount of DNA the constriction of calorimetric heat absorption peak confirms this interaction.

The investigation at high cNP/DNA ratios was not possible because of heterogeneity of solution. For this reason it would be used the other alternative methods such as UV spectrophotometry and ultracentrifugation. To determine the binding ratio we used UV/Vis spectroscopy. Formed complexes subsided and therefore the absorption of DNA in the supernatant is decreased by the adsorbed amount. In Fig. 11 the decrease of the absorption of free DNA with increasing NP concentrations can be seen. Plotting the dependence of the supernatant's absorption for different NP/[DNA] ratios (Fig. 13), allows to determine the optimal quantity of DNA connected to the NP. Earlier it was shown that the amount of DNA which could be associated with NP is 1:50 (w/w), with cationic polymer is from 1:0.4 to 1:6 (w/w) and in the case of lipid based systems is from 1:2 to 1:6 (w/w) [1]. Our experimental results show that the amount of DNA which could be associated with chitosan-coated NP with 148 nm size is 1:0.14 (w/w), or 7 g of such particles are able to attach 1 g of DNA.

It should be mentioned that the present method gives the possibility to determine the NP interaction not only with DNA, but also for other remedies. It allows determine the minimum of a substance to be delivered, required to saturate the NP.

Conclusions

Thus the carried out experiments show how necessary to study the properties of PLGA NP by physical methods. Experiments, which main purpose was to study the stability of NP, reveal some significant properties. Coating the NP with chitosan does not affect on their thermodynamic and optic behavior. It has shown that particle thermal stability depends on solvent polarity degree—as more polar solvent more is thermo stable of NP (adding the ethyl acetate decrease the stability of NP). It has been shown that the tightness breaking temperature depends on particle suspension heating rate. The minimal heating rate of existing scanning microcalorimeters is not enough for determining the tightness breaking equilibrium temperature. Study of NP stability reveals that at about 20 °C their internal volume tightness is damaged. Therefore the interior substances leakage in outer space would take place. From obtained results it has shown that the NP wholeness does not lose: the shape and size is survived even in such temperature as 150 °C, though the leak tightness is damaged. It has shown that the NP maintain their structure wholeness in a wide pH acidity interval (2.0–8.0) and not only in bidistilled or deionized water (at least in buffer with low molarity), what is important for drug transfer orally without nanoparticle tightness damage.

It was determined the amount of DNA which can be adsorbed on the surface of the NP which turned out that the optimal ratio of chitosan-coated NP to DNA is 7:1 (W_{Np}/W_{DNA}). It should be mentioned that the present method gives the possibility to determine the NP interaction not only for DNA, but also for other remedies. It allows determine the minimum of a substance to be delivered, required to saturate the NP.

References

1. Panyam J, Labhasetwar V. Biodegradable nanoparticles for drug and gene delivery to cells and tissue. Adv Drug Del Rev. 2003; 55:329–47.
2. Patil Y, Panyam J. Polymeric nanoparticles for siRNA delivery and gene silencing. Int J Pharm. 2009;367:195–203.
3. Patil Y, Toti U, Khdair A, Ma L, Panyam J. Facile single-step multifunctionalization of nanoparticles for targeted drug delivery. Biomaterials. 2009;30:859–66.
4. Bejjani RA, BenEzra D, Cohen H, Rieger J, Andrieu C, Jeanny J, et al. Nanoparticles for gene delivery to retinal pigment epithelial cells. Mol Vis. 2005;11:124–32.
5. Nishikawa M, Huang L. Nonviral vectors in the new millennium: delivery barriers in gene transfer. Hum Gene Ther. 2001;12:861–70.
6. Li S, Huang L. Nonviral gene therapy: promises and challenges. Gene Ther. 2000;7:31–4.
7. Ferber D. Gene therapy: safer and virus-free? Science. 2001;294: 1638–42.
8. Moghimi SM, Hunter AC, Murray JC. Long circulating and target-specific nanoparticles: theory to practice. Pharmacol Rev. 2001;53:283–318.
9. Douglas SJ, Davis SS, Illum L. Nanoparticles in drug delivery. Crit Rev Ther Drug Carrier Syst. 1987;3:233–61.
10. Kreuter J, Tauber U, Illi V. Distribution and elimination of poly(methyl methacrylate) nanoparticles after subcutaneous administration to rats. J Pharm Sci. 1979;68:1443–9.
11. Hasadsri L, Kreuter J, Hattori H, Iwasaki T, George JM. Functional protein delivery into neurons using polymeric nanoparticles. J Biol Chem. 2009;284:6972–81.
12. Brown MD, Schatzlein AG, Uchegbu IF. Gene delivery with synthetic (non viral) carriers. Int J Pharm. 2001;229:1–21.
13. Fievez V, Plapied L, des Rieux A, Pourcelle V, Freichels H, Wascotte V, Vanderhaeghen ML, Jerôme C, Vanderplasschen A, Marchand-Brynaert J, Schneider YJ, Préat V. Targeting nanoparticles to M cells with non-peptidic ligands for oral vaccination. Eur J Pharm Biopharm 2009; May 3 [Epub ahead of print].
14. De S, Robinson D. Polymer relationships during preparation of chitosan-alginate and poly-l-lysine-alginate nanospheres. J Control Rel. 2003;89:101–12.
15. Ricci M, Blasi P, Giovagnoli S, Perioli L, Vescovi C, Rossi C. Leucinostatin-A loaded nanospheres: characterization and in vivo toxicity and efficacy evaluation. Int J Pharm. 2004;275:61–72.
16. Muller M, Voros J, Csucs G, Walter E, Danuser G, Textor M, et al. Surface modification of PLGA microspheres. J Biomed Mater Res. 2003;66A:55–61.
17. Feng SS, Huang GF, Mu L. Nanospheres of biodegradable polymers: a system for clinical administration of an anticancer drug paclitaxel. Ann Acad Med Singapore. 2000;29:633–9.
18. Feng SS, Huang GF. Effects of emulsifiers on the controlled release of paclitaxel (Taxol) from nanospheres of biodegradable polymers. J Control Rel. 2001;71:53–69.
19. Pan J, Feng SS. Targeting and imaging cancer cells by folate decorated, "quantum dots loaded nanoparticles of biodegradable polymers". Biomaterials. 2009;30:1176–83.
20. Mu L, Feng SS. Fabrication, characterization and in vivo release of paclitaxel (Taxol) loaded poly(lactic-co-glycolic acid) microspheres prepared by spray drying technique with lipid/cholesterol emulsifiers. J Control Rel. 2001;76:239–54.
21. Mu L, Feng SS. Vitamin E TPGS used as emulsifier in the solvent evaporation/extraction technique for fabrication of polymeric nanospheres for controlled release of paclitaxel (Taxol). J Control Rel. 2002;80:129–44.
22. Labhasetwar V. Nanoparticles for drug delivery. Pharm News. 1997;4:28–31.
23. Allemann E, Leroux JC, Gurny R. Polymeric nano- and microparticles for the oral delivery of peptides and peptidomimetics. Adv Drug Del Rev. 1998;34:171–89.
24. Nishioka Y, Yoshino H. Lymphatic targeting with nanoparticulate system. Adv Drug Del Rev. 2001;47:55–64.
25. Soppimath KS, Aminabhavi TM, Kulkarni AR, Rudzinski WE. Biodegradable polymeric nanoparticles as drug delivery devices. J Contr Rel. 2001;70:1–20.
26. Hariharan S, Bhardwaj V, Bala I, Sitterberg J, Bakowsky U, Kumar R. Design of estradiol loaded PLGA nanoparticulate formulations: a potential oral delivery system for hormone therapy. Pharm Res. 2006;23:184–95.
27. Mittal G, Sahana D, Bhardwaj V, Kumar R. Estradiol loaded PLGA nanoparticles for oral administration: effect of polymer molecular weight and copolymer composition on release behavior in vitro and in vivo. J Control Rel. 2007;119: 77–85.
28. Sonaje K, Italia J, Sharma G, Bhardwaj V, Tikoo K, Kumar R. Development of biodegradable nanoparticles for oral delivery of ellagic acid and evaluation of their antioxidant efficacy against cyclosporine A-induced nephrotoxicity in rats. Pharm Res. 2007; 24:899–908.
29. Jeon HJ, Jeong YL, Jang MK, Park YH, Nah JW. Effect of solvent on the preparation of surfactant-free poly (D, L-lactide-co-glycolide) nanoparticles and norfloxacin release characteristics. Int J Pharm. 2000;207:99–108.
30. Day M, Nawaby AV, Liao X. A DSC study of the crystallization behaviour of polylactic acid and its nanocomposites. J Therm Anal Cal. 2006;86:623–9.
31. Cilurzo F, Selmin F, Liberti V, Montanari L. Thermal characterization of poly(lactide-co-glycolide) microspheres containing bupivacaine base polymorphs. J Therm Anal Cal. 2005;79:9–12.
32. Anderson JM, Shive MS. Biodegradation and biocompatibility of PLA and PLGA microspheres. Adv Drug Del Rev. 1997;28:5–24.
33. Jain RA. The manufacturing techniques of various drug loaded biodegradable poly (lactide-co-glycolide) (PLGA) devices. Biomaterials. 2000;21:2475–90.
34. Langer R. Tissue engineering: a new field and its challenges. Pharm Res. 1997;14:840–1.
35. Uhrich KE, Cannizzaro SM, Langer RS, Shakeshelf KM. Polymeric systems for controlled drug release. Chem Rev. 1999; 99:3181–98.
36. Vert M, Schwach G, Engel R, Coudane J. Something new in the field of PLA/GA bioresorbable polymers? J Control Rel. 1998; 53:85–92.
37. Hans MK, Lowman AM. Biodegradable nanoparticles for drug delivery and targeting. Curr Opin Solid State Mater Sci. 2002;6: 319–27.
38. Sahoo SK, Panyam J, Prabha S, Labhasetwar V. Residual polyvinyl alcohol associated with poly(D, L-lactide-co-glycolide) nanoparticles affects their physical properties and cellular uptake. J Contr Rel. 2002;82:105–14.
39. Jawahar N, Eagappanath T, Venkatesh N, Jubie S, Samanta MK. Preparation and characterisation of PLGA-nanoparticles containing an anti-hypertensive agent. Int J Pharm Tech Res. 2009;1: 390–3.
40. Bala I, Haribaran S, Kumar R. PLGA nanoparticles in drug delivery: the state of the art. Crit Rev Ther Drug Carrier Syst. 2004;21:387–422.
41. Hyon SH. Biodegtadable poly(lactic acid) microspheres for drug delivery systems. Yonsei Med J. 2000;41:720–34.
42. Hanafusa S, Matsusue Y, Yasunaga T, Yamamuro T, Oka M, Shikinami Y, et al. Biodegradable plate fixation of rabbit femoral shaft osteotomies. A comparative study. Clin Orthop Relat Res. 1995;315:262–71.

43. Matsusue Y, Hanafusa S, Yamamuro T, Shikinami Y, Lkada Y. Tissue reaction of bioabsorbable ultra high strength poly (L-lactide) rod. A long-term study in rabbits. Clin Orthop Relat Res. 1995;317: 246–53.
44. Mooney DJ, Sano K, Kaufmann PM, Majahod K, Schloo B, Vacanti JP, et al. Long-term engraftment of hepatocytes transplanted on biodegradable polymer sponges. J Biomed Mater Res. 1997;37:413–20.
45. Eiselt P, Kim BS, Chacko B, Isenberg B, Peters MC, Greene KG, et al. Development of technologies aiding large-tissue engineering. Biotechnol Prog. 1998;14:134–40.
46. Cartiera MS, Johnson KM, Rajendran V, Caplan MJ, Saltzman WM. The uptake and intracellular fate of PLGA nanoparticles in epithelial cells. Biomaterials. 2009;30:2790–8.
47. Leong KW, Langer R. Polymeric controlled drug delivery. Adv Drug Del Rev. 1987;1:33–199.
48. Park TG. Degradation of poly(lactide-co-glycolide acid) microspheres: effect of copolymer composition. Biomaterials. 1995;16: 1123–30.
49. Hedley ML, Curley J, Urban R. Microspheres containing plasmid-encoded antigens elicit cytotoxic T-cell responses. Nat Med. 1998;4:365–8.
50. Lin SY, Chen KS, Teng HH, Li MJ. In vitro degradation and dissolution behaviours of microspheres prepared by three low molecular weight polyesters. J Microencapsul. 2000;17:577–86.
51. Brannon-Peppas L. Recent advances on the use of biodegradable microparticles and nanoparticles in controlled drug delivery. Int J Pharm. 1995;116:1–9.
52. Görner T, Gref R, Michenot D, Sommer F, Tran MN, Dellacherie E. Lidocaine-loaded biodegradable nanosperes. I. Optimization of the drug incorporation into the polymer matrix. J Contr Rel. 1999;57:259–69.
53. Burkersroda FV, Schedl L, Göpferich A. Why degradable polymers undergo surface erosion or bulk erosion. Biomaterials. 2002;23:4221–31.
54. Kneuer C, Sameti M, Haltner EG, Schiestel T, Schirra H, Schmidt H, et al. Silica nanoparticles modified with aminosilanes as carriers for plasmid DNA. Int J Pharm. 2000;196:257–61.
55. Kneuer C, Sameti M, Bakowsky U, Schiestel T, Schirra H, Schmidt H, et al. A nonviral DNA delivery system based on surface modified silica-nanoparticles can efficiently transfect cells in vitro. Bioconjug Chem. 2000;11:926–32.
56. Florence AT, Sakthivel T, Toth I. Oral uptake and translocation of a polylysine dendrimer with a lipid surface. J Control Rel. 2000;65:253–9.
57. Ramaswamy C, Sakthivel T, Wilderspin AF, Florence AT. Dendriplexes and their characterization. Int J Pharm. 2003;254: 17–21.
58. Pouton CW, Lucas P, Thomas BJ, Uduehi AN, Mikroy DA, Moss SH. Polycation-DNA complexes for gene delivery: a comparison of the biopharmaceutical properties of cationic polypeptides and cationic lipids. J Control Rel. 1998;53:289–99.
59. Ramsay E, Gumbleton M. Polylysine and polyornithine gene transfer complexes: a study of complex stability and cellular uptake as a basis for their differential in vitro transfection efficiency. J Drug Target. 2002;10:1–9.
60. Oupicky D, Konak C, Ulbrich K, Wolfert MA, Seymour LW. DNA delivery systems based on complexes of DNA with synthetic polycations and their copolymers. J Control Rel. 2000; 65:149–71.
61. Blacklock J, You YZ, Zhou QH, Mao G, Oupicky D. Gene delivery in vitro and in vivo from bioreducible multilayered polyelectrolyte films of plasmid DNA. Biomaterials. 2009;30: 939–50.
62. Wagner E, Plank C, Zatloukal K, Cotton M, Birnstiel ML. Influenza virus hemagglutinin HA-2 N-terminal fusogenic peptides augment gene transfer by transferrin-polylysine-DNA complexes: toward a synthetic virus-like gene-transfer vehicle. Proc Natl Acad Sci USA. 1992;89:7934–8.
63. Fischer D, Bieber T, Li Y, Elsasser HP, Kissel T. A novel nonviral vector for DNA delivery based on low molecular weight, branched polyethylenimine: effect of molecular weight on transfection efficiency and cytotoxicity. Pharm Res. 1999;16: 1273–9.
64. Kunath K, Harpe A, Fischer D, Petersen H, Bickel U, Voigt K, et al. Low-molecular-weight polyethylenimine as a non-viral vector for DNA delivery: comparison of physicochemical properties, transfection efficiency and in vivo distribution with high-molecular-weight polyethylenimine. J Control Rel. 2003;89:113–25.
65. Singh M, Briones M, Ott G, O'Hagan D. Cationic microparticles: a potent delivery system for DNA vaccines. Proc Natl Acad Sci USA. 2000;97:811–6.
66. Singh M, Ott G, Kazzaz J, Ugozzoli M, Briones M, Donnelly J, et al. Cationic microparticles are an effective delivery system for immune stimulatory CpG DNA. Pharm Res. 2001;18:1476–9.
67. Singh M, Vajdy M, Gardner J, Briones M, O'Hagan D. Mucosal immunization with HIV-1 gag DNA on cationic microparticles prolongs gene expression and enhances local and systemic immunity. Vaccine. 2001;20:2–594.
68. Smith JG, Wedeking T, Vernachio JH, Way H, Niven RW. Characterization and in vivo testing of a heterogeneous cationic lipid-DNA formulation. Pharm Res. 1998;15:1356–63.
69. Olbrich C, Bakowsky U, Lehr C-M, Muller RH, Kneuer C. Cationic solid-lipid nanoparticles can efficiently bind and transfect plasmid DNA. J Control Rel. 2001;77:345–55.
70. Oberle V, Bakowsky U, Zuhorn IS, Hoekstra D. Lipoplex formation under equilibrium conditions reveals a three step mechanism. Biophys J. 2000;79:1447–54.
71. Mahato RI, Kawabata K, Nomura T, Takakura Y, Hashida M. Physicochemical and pharmacokinetic characteristics of plasmid DNA/cationic liposome complexes. J Pharm Sci. 1995;84:1267–71.
72. Cui Z, Mumper RJ. Plasmid dna-entrapped nanoparticles engineered from microemulsion precursors: in vitro and in vivo evaluation. Bioconjug Chem. 2002;13:1319–27.
73. Farhood H, Serbina N, Huang L. The role of dioleyl phosphatidylethanolamine in cationic liposome mediated gene transfer. Biochim Biophys Acta. 1995;1235:289–95.
74. Sternberg B, Hong K, Zheng W, Papahadjopoulos D. Ultrastructural characterization of cationic liposome-DNA complexes showing enhanced stability in serum and high transfection activity in vivo. Biochim Biophys Acta. 1998;1375:23–35.
75. Meyer O, Kirpotin D, Hong K, Sternberg B, Park J, Woodle M, et al. Cationic liposomes coated with polyethylene glycol as carriers for oligonucleotides. J Biol Chem. 1998;273:15621–7.
76. Behr JP, Demeneix B, Loeffler JP, Perez-Mutul J. Efficient gene transfer into mammalian primary endocrine cells with lipopolyamine-coated DNA. Proc Natl Acad USA. 1989;86:6982–6.
77. Torchilin VP, Levchenko TS, Rammohan R, Volodina N, Papahadjopoulos-Sternberg B, D'Souza GG. Cell transfection in vitro and in vivo with nontoxic TAT peptide–liposome–DNA complexes. Proc Natl Acad Sci USA. 2003;100:1972–7.
78. Rädler J, Koltover I, Salditt T, Safinya C. Structure of DNA–cationic liposome complexes: DNA intercalation in multilamellar membranes in distinct interhelical packing regimes. Science. 1997;7:810–4.
79. Mrevlishvili G, Kankia B, Mdzinarashvili T, Brelidze T, Khvedelidze M, Metreveli N, et al. Liposome–DNA interaction: microcalorimetric study. Chem Phys Lipids. 1998;94:139–43.
80. Zuzzi S, Onori G, Cametti C. Thermal stability of DNA in DNA-induced dotap liposome aggregates. J Therm Anal Cal. 2008;93: 527–33.

81. Cui Z, Mumper RJ. Plasmid DNA-entrapped nanoparticles engineered from microemulsion precursors: in vitro and in vivo evaluation. Bioconjug Chem. 2002;13:1319–27.
82. Kumar R, Bakowsky U, Lehr C-M. Preparation and characterization of cationic PLGA nanospheres as DNA carriers. Biomaterials. 2004;25:1771–7.
83. Kumar R, Mohapatra SS, Kong X, Jena P, Bakowsky U, Lehr C-M. Cationic poly(lactide-co-glycolide) nanoparticles as efficient in vivo gene transfection agents. J Nanosci Nanotechnol. 2004;4:990–4.
84. Zoua W, Liua C, Chena Z, Zhang N. Studies on bioadhesive PLGA nanoparticles: a promising gene delivery system for efficient gene therapy to lung cancer. Int J Pharm. 2009;370:187–95.
85. Lira AAM, Nanclares DMA, Federman Neto A, Marchetti JM. Drug-polymer interaction in the all-*trans* retinoic acid release from chitosan microparticles. J Therm Anal Cal. 2007;87:899–903.
86. Haas J, Ravi K, Borchard G, Bakowsky U, Lehr C-M. Preparation and characterization of chitosan and trimethyl-chitosan-modified poly-(ε-caprolactone) nanoparticles as DNA carriers. AAPS Pharm Sci Tech. 2005;6:22–30.
87. Luengo J, Weiss B, Schneider M, Ehlers A, Stracke F, König K, et al. Influence of nanoencapsulation on human skin transport of flufenamic acid. Skin Pharmacol Physiol. 2006;19:190–7.
88. Xu P, Gullotti E, Tong L, Highley CB, Errabelli DR, Hasan T, et al. Intracellular drug delivery by poly(lactic-co-glycolic acid) nanoparticles, revisited. Mol Pharm. 2009;6:190–201.
89. Nafee N, Taetz S, Schneider M, Schaefer U, Lehr C-M. Chitosan-coated PLGA nanoparticles for DNA/RNA delivery: effect of the formulation parameters on complexation and transfection of antisense oligonucleotides. Nanomedicine: nanotechnology. Biol Med. 2007;3:173–83.
90. Privalov PL, Potekhin SA. Scanning microcalorimetry in studying temperature-induced changes in proteins. Meth Enzim. 1986; 131:4–51.
91. De S, Robinson DH. Particle size and temperature effect on the physical stability of PLGA nanospheres and microspheres containing Bodipy. AAPS PharmSciTech. 2004;5:1–7.